International Journal of Mechanical, Industrial and Aerospace Sciences
ISSN: 2517-9950
Vol:8, No:2, 2014

Dynamic Stall Vortex Formation of OA-209 Airfoil at Low Reynolds Number

Aung Myo Thu, Sang Eon Jeon, Yung Hwan Byun, Soo Hyung Park

***Abstract*—**The unsteady flow field around oscillating OA-209 airfoil at a Reynolds number of 3.5×105 were investigated. Three different reduced frequencies were tested in order to see how it affects the hysteresis loop of an airfoil. At a reduced frequency of 0.05 the deep dynamic stall phenomenon was observed. Lift overshooting was observed as a result of dynamic stall vortex (DSV) shedding. Further investigation was carried out to find out the cause of DSV formation and shedding over airfoil. Particle image velocimetry (PIV) and CFD tools were used and it was found out that dynamic stall separation (DSS), which is separated from leading edge separation (LES) and trailing edge separation (TES), triggered the dynamic stall vortex (DSV).

***Keywords*—**Airfoil Flow, CFD, PIV, Dynamic Stall, Flow Separation.

I. Introduction

AN airfoil that experiences an unsteady change in angle of attack which pushes it beyond static stall angle is known to increase in lift while maintaining lift curve slope. This kind of phenomenon has also been seen on helicopter rotors which experiences sinusoidal variation in blade incidence angle as it rotates around the azimuth. As angle of attack of an airfoil increases, the more lift is attained and finally reaches a lift peak where the lift is totally lost.

Simultaneously, a vortex is formed over the airfoil and grows larger. Finally, this vortex is shed over the airfoil and the airfoil experiences negative moment. This is the general flow features of dynamic stall observed in two dimensional flow experiments.

Dynamic stall largely affects the aerodynamic performance of fluid machinery such as gas turbines, helicopter blades, flapping wings, wind turbines and so on. A typical dynamic stall process can be categorized into four stages: attached flow, dynamic stall vortex (DSV) development, shedding of the leading edge vortex, and reattachment of the flow to the suction surface.

There have been numerous attempts on dynamic stall problems in order to understand the complex flow phenomenon. McCroskey [4] reviewed the phenomenon of dynamic stall as early as in 1981. Recently, Shengyi Wang [3] has analyzed deep dynamic stall problems at relatively low Reynolds number using different turbulence modeling techniques and Kobra Gharali [2] has done some PIV experiment on SD7037 airfoil dynamic stall case. San Eon Jeon [1] and Geissler [5], [6] put their effort on OA-209 airfoil. However, the physics of highly non linear behavior of dynamic stall has yet not fully understood especially at a low Reynolds number of the order of 10^5. Most of the previous researches have been focused on high Reynolds number region, such as 10^6, which represents flow in helicopter blades. For this kind of high Reynolds number flows, most of the airfoils experience leading edge dynamic stall. At a relatively low Mach number flows, trailing edge stall is dominant. The strong adverse pressure gradient causes the trailing edge separation whereas the burst of the laminar separation bubble (LSB) is the main reason of leading edge dynamic stall. There are a lot of factors influencing the physics of dynamic stall, such as leading edge shape, amplitude, mean angle of attack, reduced frequency and flow velocity. In this study the effect of reduced frequency on dynamic stall behavior is discussed. The DSV formation process is investigated experimentally (PIV) and numerically.

Aung Myo Thu, Sang Eon Jeon, Yung Hwan Byun, and Soo Hyung Park are with the Konkuk University, Seoul, Republic of Korea (e-mail: ricky2020@gmail.com, eonman@ korea.com, yhbyun@konkuk.ac.kr, pish@ konkuk.ac.kr, respectively).

II. Numerical and Experimental Methods

For numerical calculations, Navier-Stokes equations and the shear stress transport (SST) *k*-ω turbulence model in combination with Langtry [7] and Menter's [8] transition transport equations were used. Reynolds-averaged Navier-Stokes equations and shear stress transport turbulence equations were used as a baseline governing equations, for dynamic stall flows, the Menter et al.'s γ-Re_θ transition model [8] was used in order to account for laminar-turbulent transition. The C-type grid system was used with 512x120 cells in the stream wise and wall normal directions. Far field boundaries were 40 chord lengths away from the quarter chord position of the airfoil. The cell spacing for the first grid point from the wall boundary is $2.5x10^{-6}$ c (chord length). This length is sufficient to resolve the viscous sub layer in the turbulent boundary layer.

The experiments were conducted in the Subsonic Wind Tunnel (SWT) at Aerodynamic Analysis and Design Laboratory in Konkuk University, Korea. The AADL SWT can be operated in two options: open or closed circuit. It has two test sections: the first test section is 1-m square and 3.5-m long and the second one is 2.2-m (W) × 2-m (H) ×9-m (L).

The first test section can be operated up to 45 m/s while the second one can be achieved 10 m/s. The schematic of OA-209 airfoil model used for this experiment is shown in Fig. 1. The wind tunnel speed was M=0.1 and the model was mounted in the centre of the test section.

The PIV experiments were conducted to see the flow field of OA-209 airfoil. Quantel Nd:Yag Laser 145 was used to

illuminate the flow field. It can emit 532nm wavelength of laser with maximum power of 145 mJ and can run up to 15 Hz repetition rate. The flow is seeded with PivPar30 particle generator. The DEHS aerosols with the size of 1μm were seeded pumping through particle generator. The images were captured with PCO 1600 CCD camera which has 14 bit dynamic range and 1600 x 1200 pixel resolutions. The camera, laser and airfoil were synced with ILA synchronizer.

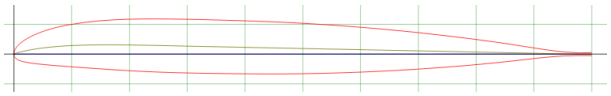

Fig. 1 OA-209 airfoil

III. Results and Discussions

The sinusoidal pitching motion of OA-209 airfoil is defined as $\alpha = \alpha_0 + \alpha_1 \sin(2kt^*)$. Three different reduced frequencies (0.0125, 0.025, 0.05) were tested. The mean angle of attack studied in this case was 10 degrees and the amplitude was 14 degrees. The flow Reynolds number investigated was 3.5×10^5. Fig. 2 shows the hysteresis loops of OA-209 airfoil at three different reduced frequencies, k=0.0125, 0.025 and 0.05. The lift variations are nearly similar in the linear region. It is common to see the increases in lift and delay of flow reattachment as the reduced frequency increases.

It's also apparent that the recovery from the stall event is further delayed and the hysteresis loops enlarged as the reduced frequency is increased. The lift overshoot due to dynamic stall vortex shedding can be seen only at the reduced frequency of 0.05 and the secondary peak was also captured in that case.

The skin friction plots of OA-209 airfoil at different angle of attacks are shown in Fig. 3. Negative skin friction means the place where separation exists. The laminar separation bubble had been observed on the airfoil surface since the initial stage of the stall process. At angle of attack of 10.8 degrees, large laminar separation bubble is observed. As angle of attack is increased to 17.4, LSB size gets smaller and moves forward. Trailing edge separation is also detected there. At the angle of attack of 18.2 degrees, a particular flow separation appears starting at about 25 percent of chord. This separation bubble can also be seen in the vorticity contour plot (which got from CFD) in Fig. 4. This particular separation is dynamic stall separation (DSS) and the presence of it is further confirmed by PIV result in Fig. 5. The complex interaction of DSS and TES were captured in PIV images.

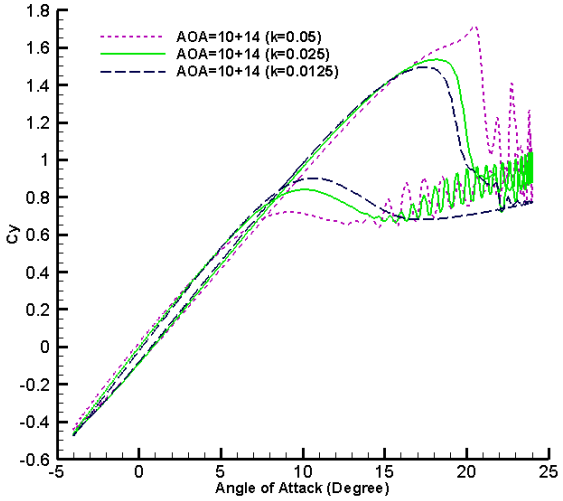

Fig. 2 Effect of reduced frequency on hysteresis loop

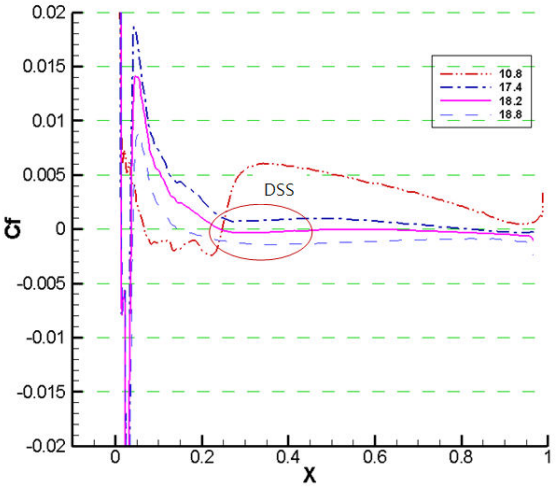

Fig. 3 Skin friction plots of OA-209 airfoil at AOA=10+14 sin(2kt*), k=0.05

After DSS was observed over airfoil, airfoil experienced full separation. That can be seen in Fig. 3-separation region covers 80% of chord at 18.8˚. This is the presence of DSV which increases lift in hysteresis loop. When angle of attack is reached to 20˚, fully developed DSV is trying to detach from airfoil surface. This DSV shedding process can be vividly seen in Figs. 6 and 7. Another counter rotating vortex, which emerge from airfoil trailing edge, is also observed. Airfoil experienced lift stall after shedding of DSV into the wake.

The shedding of the dynamic stall vortex increases the pressure on the upper surface of airfoil and then causes a fall in the lift coefficient. As angle of attack was further increased, the shedding of the secondary vortex, which led to form a secondary peak in hysteresis curve, was observed. Secondary small vortex shedding was visualized by CFD and PIV results shown in Figs. 8 and 9. The shedding of the secondary vortex over airfoil decreases lift again and airfoil experienced second stall again.

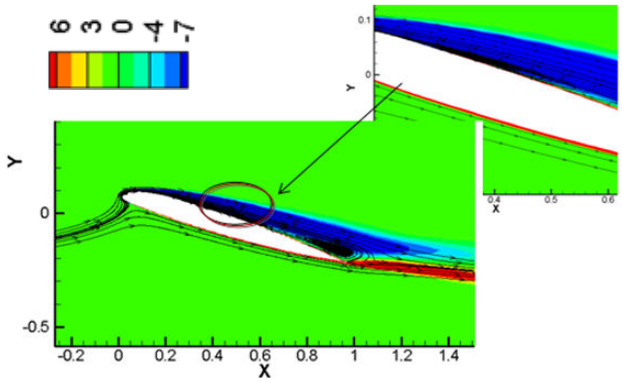

Fig. 4 Vorticity contour superimposed with streamlines of CFD at 18.2˚ upstroke

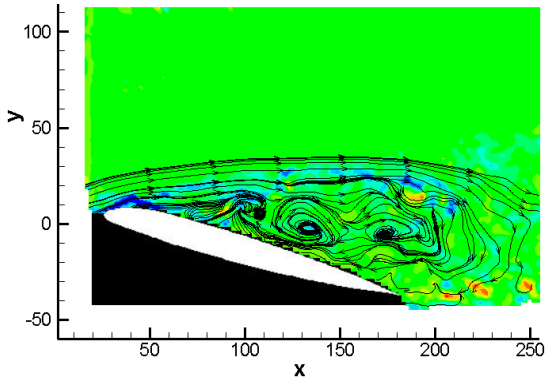

Fig. 5 Vorticity contour superimposed with streamlines of PIV at 18.2˚ upstroke

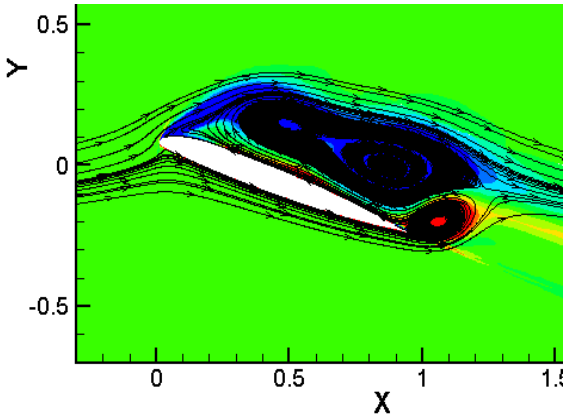

Fig. 6 Vorticity contour superimposed with streamlines of CFD at 20˚ upstroke

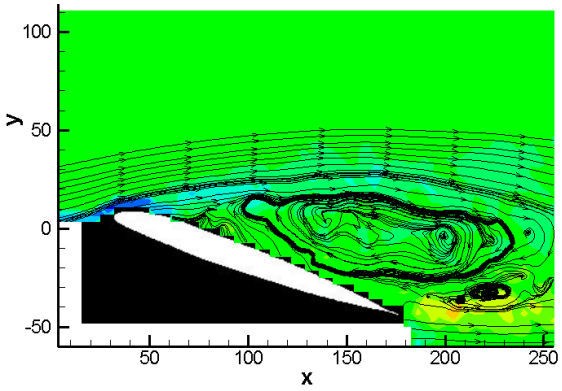

Fig. 7 Vorticity contour superimposed with streamlines of PIV at 20˚ upstroke

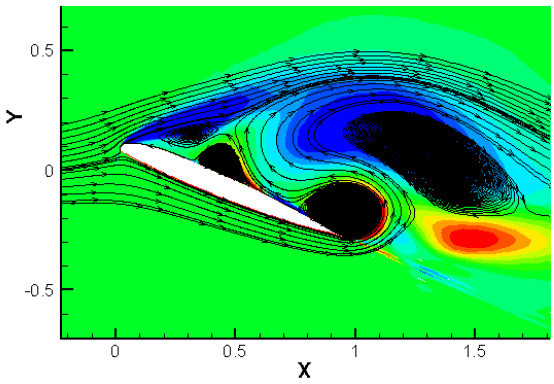

Fig. 8 Vorticity contour superimposed with streamlines of CFD at 23˚ upstroke

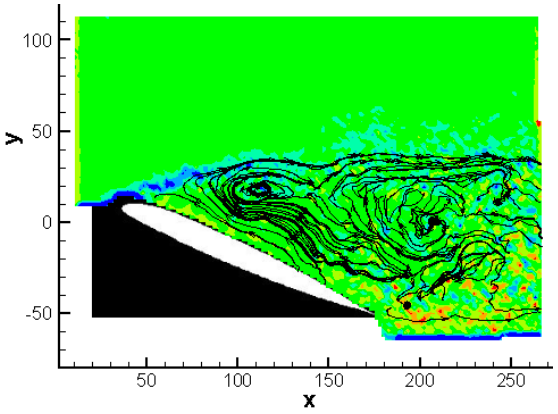

Fig. 9 Vorticity contour superimposed with streamlines of PIV at 23˚ upstroke

IV. Conclusions

The dynamic stall phenomena of a pitch oscillating OA-209 airfoil at a relatively low Reynolds number of 3.5×10^5 was studied by CFD and PIV. Three different cases were tested to see its effect on dynamic stall process. The common features of reduced frequency effect, such as delay in the stall event, increase in lift and delay in flow reattachment, were observed. The laminar separation bubble was observed since the initial

stage of dynamic stall process for the present low Reynolds number airfoil. The main reason for this test campaign is to investigate the reason behind the creation of DSV at low Reynolds number. According to the author's finding, DSV is formed by rapid merging of TES and DSS. The primary DSV shedding and secondary vortex shedding, which cause primary and secondary stall in lift hysteresis loop, was also observed.

REFERENCES

[1] Sang Eon Jeon, Soo Hyung Park, Yung Hwan Byun, Kai Richter, Wolfgagn Geissler, "Numerical investigation of boundary layer separation over an airfoil during dynamic stall," *European Rotorcraft Forum 2012*, 4-6 September 2012, Amsterdam, Netherland.

[2] Kobra Gharali, Mingyao Gu, David A. Johnson, "A PIV Study of a low Reynolds number pitch oscillating SD7037 Airfoil in dynamic stall with CFD comparison", 16th International Symposium on Applications of Laser Techniques to Fluid Mechanics, 9-12 July, 2012, Lisbon, Portugal.

[3] Shengyi Wang, Derek B. Ingham, Lin Ma, Mohamed Pourkashanian, Zhi Tao, "Turbulence modeling of deep dynamic stall at relatively low Reynolds number". Journal of Fluids and Structures, 2012. B. Smith, "An approach to graphs of linear forms (Unpublished work style)," unpublished.

[4] W. J. McCroskey, "The phenomenon of dynamic stall", NASA TM81264, 1981.

[5] W. Geissler, Dietz, G., Mai, H., Bosbach, J., and Richard, H., "Dynamic stall and its passive control investigation on the OA209 airfoil section," 31st European Rotorcraft Forum, Florence, Italy, September, 2005.

[6] W. Geissler, Haselmeyer, H., "Investigation of dynamic stall onset," Aerospace Science and Technology, Volume 10, Issue 7, October, 2006.

[7] R.Langtry, F.R.Menter, "Correlation based transition modeling for unstructured parallelized computational fluid dynamics codes," AIAA Journal, Vol.47,No.12,pp.2894-2906,2009.

[8] F.R.Menter, "Two-equation eddy-viscosity turbulence models for engineering applications," AIAA Journal, Vol.32, No.8, pp.1598-1605,1994.